# Structures and stability of defect-free multiwalled carbon toroidal rings

P. Liu, Y. W. Zhang, and C. Lu

Citation: Journal of Applied Physics **98**, 113522 (2005); doi: 10.1063/1.2138371
View online: https://doi.org/10.1063/1.2138371
View Table of Contents: http://aip.scitation.org/toc/jap/98/11
Published by the American Institute of Physics

# Structures and stability of defect-free multiwalled carbon toroidal rings

P. Liu
*Institute of High Performance Computing, Singapore 117528*

Y. W. Zhang[a)]
*Department of Materials Science and Engineering, National University of Singapore, Singapore 119260*

C. Lu
*Institute of High Performance Computing, Singapore 117528*

(Received 3 June 2005; accepted 26 October 2005; published online 14 December 2005)

Atomistic simulations of the structures and stability of defect-free multiwalled carbon toroidal rings were performed using the second-generation empirical bond-order potential and a Morse-type van der Waals potential. It was found that a multiwalled toroidal ring improves the structural stability over its outermost single-walled counterpart, implying a stabilizing effect from the inner rings. This can be explained by the superlinear relation between the critical ring diameter and its tube diameter existing in single-walled rings. However, the findings that the critical diameter of an armchair ring is larger than that of a zigzag ring with the same tube diameters, and that the inclusion of torsion exhibits a negative effect on the stability of a multiwalled ring, are in contrast to that of a single-walled nanoring. In addition, the instability of a multiwalled nanoring always starts with the formation of many short-wavelength ripples on the compressed side of the outermost tube. Subsequently, some of the ripples develop into buckles, resulting in buckling failures. © *2005 American Institute of Physics*. [DOI: 10.1063/1.2138371]

## INTRODUCTION

Carbon nanotubes are ideal candidates for the basic building blocks of nanoelectronic and nanomechanical devices due to their unique electronic and mechanical properties.[1] Nanorings, which are a variant of nanotubes, have recently attracted great research interest due to their unusual electronic and magnetic properties.[2,3] So far both single-walled[4–8] and multiwalled[9] carbon rings have been synthesized experimentally. It was found that the synthesized carbon rings have a relatively large diameter in the range of 200–700 nm, exhibiting either a closed and seamless toroidal shape involving the formation of covalent bonds,[4,8] or a coiled shape stabilized by van der Waals (vdW) forces.[5–7,9]

To improve the electronic and magnetic performance of nanorings, it is highly desirable to reduce the diameter and the number of defects (pentagons and heptagons) of the carbon toroidal rings. One way to achieve this is to geometrically fold a defect-free straight nanotube into a circular ring by covalently bonding its two ends. The advantages of this method are that there is no ambiguity in the boundary condition and no defects such as pentagons or heptagons are introduced.[10–20] The nanotube must be bent before the formation of bonds, to allow its two ends to join. Thus the strain energy arising from bending the straight nanotube into a closed ring forms the formation energy barrier. For a fixed tube diameter, the smaller the nanoring diameter, the higher the strain energy per atom and thus the higher the energy barrier.[16] Hence external work must be done to overcome the elastic energy barrier. The smallest stable nanoring diameter should depend on the competition between the strain energy increase and the end-connection bonding energy reduction, leading to a critical diameter of the toroidal ring for a given diameter and helicity of nanotube.[10–14]

The structures and stability of single-walled toroidal carbon nanorings were recently investigated by Liu *et al.*,[10] Han,[11] Huhtala *et al.*,[12,13] and Hod *et al.*[14] using large-scale molecular-dynamics simulations. It was found that for a fixed tube diameter, indeed there is a critical ring diameter above which the toroidal ring is stable whereas below which the ring is unstable; the instability arises in a ripple formation and buckling.[10–14] The geometrical structure, electronic structure, and energy of small single-walled carbon toroidal rings were investigated by means of a tight-binding and semiempirical quantum chemical approach.[15,16] Continuum elastic theories were also applied to study the formation mechanism and stability of single-walled carbon tori.[17–20] It appears that although the structure and stability of single-walled rings have been analyzed over the past years, much less is known about the structures and stability of defect-free multiwalled toroidal rings. For the multiwalled toroidal rings, it is expected that the vdW interactions between ring walls will be of importance and thus affect their structures and stability.

A common way to form a defect-free single-walled toroidal nanoring is to geometrically bend a straight armchair or zigzag nanotube into a circular ring by connecting its two ends, and subsequently the geometrically bent nanoring is then subjected to energy relaxation.[10–14] In the present work, the same method was used to form defect-free multiwalled carbon toroidal rings. The objective of this study is to systematically investigate the structures and stability of defect-free carbon toroidal rings, with an emphasis on the influence

[a)]Author to whom correspondence should be addressed; FAX: 65-67763604; electronic mail: msezyw@nus.edu.sg

 

of the number of walls, the interwall distance, and the diameter, length, helicity, and torsion of the nanotubes.

## FORMULATIONS

To simulate the formation and stability of a multiwalled carbon toroidal ring, the second-generation reactive empirical bond-order (2GREBO) potential[21] was used for the atomic interactions within a wall, and a Morse-type vdW potential based on a local-density approximation was used for the atomic interactions between walls.[22] The combined form of the binding energy consists of the 2GREBO potential and the vdW potential and can be written as

$$E_B = \sum_i \sum_{i>j} [V_R(r_{ij}) - B_{ij} V_A(r_{ij}) + V_{\mathrm{vdW}}(r_{ij})],$$

where $V_R$ is the core-core pair-additive repulsive interaction, $V_A$ is the valence electron-core pair-additive attractive interaction, $r_{ij}$ is the distance between atoms $i$ and $j$, for $i,j \in [1,n]$, where $n$ is the total number of atoms, $B_{ij}$ is the many-body bond-order term, and $V_{\mathrm{vdW}}$ is the vdW energy. The 2GREBO potential used improved analytical functions and an extended database, leading to an improved description of the chemical and mechanical properties for hydrogen molecules, diamond, and fullerene structures.[21,23,24] In the present atomistic simulations, the Verlet integration scheme in combination with velocity damping was used to perform energy minimization. A time step size of $1.05 \times 10^{-15}$ s was used.

## RESULTS AND DISCUSSIONS

The structure and stability of defect-free multiwalled carbon toroidal rings depend on the system parameters, such as the number of walls, the wall-wall distance, the diameter, length, helicity, and torsion of the nanotubes. The present study aims to understand how these system parameters affect the structure and stability of these defect-free toroidal carbon rings. The diameter of the geometrically folded ring before energy relaxation, $D$, is related to the length of its corresponding straight nanotube $L$, by $D=L/\pi$. $D_C$ is defined as the critical diameter of instability of the ring during energy relaxation. Torsion refers to the axial rotation of the cross section of one end of a straight nanotube by 360° relative to the other end, followed by geometrically bending the rotated nanotubes into a circular ring connecting its two ends.

To compare the influences of system parameters on the structure and stability, we first investigated the stability of single-walled rings obtained by bending single-walled nanotubes. During the energy relaxation, the potential energy per atom gradually decreases and finally approaches a constant for a stable nanoring, whereas for an unstable ring, the potential energy per atom decreases substantially and subsequently suffers a sudden drop due to buckling. For a single-walled ring with a fixed nanotube configuration (diameter, helicity, and torsion), our simulations showed that there is a critical ring diameter (or tube length), above which the ring is stable whereas below which the ring is unstable; this result is consistent with previous studies.[10–14] A large number of simulations were conducted here to estimate the critical diameter $D_C$ for nanorings with armchair and zigzag configurations and with different tube diameters. Figure 1 shows the variations of the approximate critical diameter $D_C$ of a single-walled nanoring with its nanotube diameter $d$ for the following three situations: armchair configuration without torsion, armchair configuration with torsion, and zigzag configuration with torsion. These single-walled nanorings have configurations (3,3), (4,4), (5,5), and (6,6) for the armchair type and (5,0), (7,0), (9,0), and (10,0) for the zigzag type.

Figure 2 shows the relationship of the approximate critical diameter $D_C$ of the double-walled nanoring versus its inner nanotube diameter $d$ for the following three situations: armchair configuration without torsion, armchair configuration with torsion, and zigzag configuration without torsion. These double-walled nanorings have configurations of (3,3)+(8,8), (4,4)+(9,9), (5,5)+(10,10), and (6,6)+(11,11) for the armchair type and (5,0)+(14,0), (7,0)+(16,0), (9,0)+(18,0), and (10,0)+(19,0) for the zigzag type. It should be noted that the equilibrium wall-wall distance of 0.34 nm was used for these double-walled nanorings.

A comparison between the single-walled and double-walled cases allows several observations to be made: (I) The critical diameters for both single-walled and multiwalled nanorings can be as low as a few nanometers which are significantly smaller than 200–700 nm observed in the experiments.[4–8] The reason for this huge difference is due to the strain energy barrier for nanoring formation. To overcome the strain energy barrier, far-from-equilibrium processing conditions are required. However, these experiments were performed at near-equilibrium conditions, and thus could only lead to the nanorings with much larger diameters.[4–8] (II) The critical diameter $D_C$ of the nanoring increases with an increase in the nanotube diameter $d$, which is consistent with the simulation and analysis results in Refs. 9–18. This observation is generic, which is applicable to both single-walled and multiwalled nanotubes with both armchair and zigzag configurations with or without torsion. The underlying reason for this can be explained by elastic bending theory: for the same value of ring diameter $D$, the larger the nanotube diameter $d$, the higher the atomic stress, thus the higher the strain energy per atom. The ring loses its stability when the increase in strain energy exceeds the reduction in the end-connection bonding energy. (III) For a single-walled nanoring with a fixed nanotube diameter, the critical diameter of the nanoring with torsion is smaller than that without torsion, as shown in Fig. 1, indicating that torsion has a stabilizing effect on the stability of a single-walled nanoring. For example, the critical diameters of the (4,4) configuration with and without torsion are approximately 3.93 and 7.86 nm, respectively. However, for a double-walled nanoring with fixed nanotube diameters, the critical diameter of the nanoring with torsion is larger than that without torsion, as shown in Fig. 2, indicating that torsion has a destabilizing effect on the stability of a multiwalled nanoring. For ex-

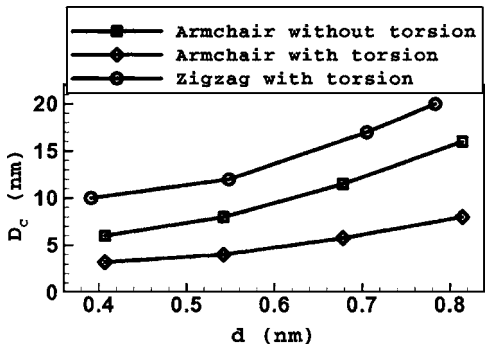


FIG. 1. Critical nanoring diameter $D_C$ vs nanotube diameter $d$ for single-walled nanorings with armchair configurations without torsion, armchair configurations with torsion, and zigzag configurations with torsion.

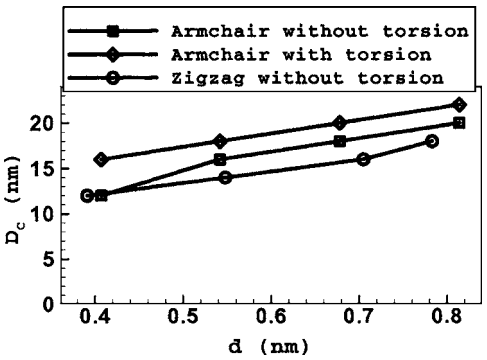


FIG. 2. Critical nanoring diameter $D_C$ vs nanotube diameter $d$ for double-walled nanorings with armchair configurations without torsion, armchair configurations with torsion, and zigzag configurations without torsion.

ample, the critical diameters of the $(4,4)+(9,9)$ configuration with and without torsion are approximately 17.67 and 15.72 nm, respectively. By examining the evolution of the cross sections of the multiwalled rings along the circumferential direction, we found that the changes of both inner and outer cross sections are not synergetic. During the bending of a torsional nanotube, the atomic arrangements at different nanotube cross sections are different, causing a different response to the bending moment. Thus there are nonuniform expansions and contractions of cross sections along the circumferential direction. These nonuniform deformations of cross sections change the wall-wall distance between the inner and outer walls, resulting in nonuniform vdW interactions, which in turn destabilize the local configuration and result in local buckling failure. (IV) The critical diameter of a single-walled armchair nanoring is smaller than its zigzag counterpart with the same nanotube diameter, as shown in Fig. 1, indicating that the armchair configuration is more stable than the zigzag configuration; this result is consistent with previous studies.[12,13] However, for a double-walled nanoring, the critical diameter of an armchair ring is larger than its zigzag counterpart with the same nanotube diameter (Fig. 2), indicating that the zigzag configuration is more stable than the armchair configuration. During the relaxation of a double-walled ring, the diameter of both inner and outer rings shrinks gradually (more discussion will be given on this shortly). It was found that the shrinking velocities and magnitudes between the inner and outer rings are different for armchair and zigzag configurations. For the zigzag type, the inner ring shrinks slightly faster and larger than the outer ring, thus the wall-wall distance at the compressive side of the rings decreases while the repulsive vdW forces increase. The inner ring provides support through the repulsive vdW forces, thus restraining the development of ripples in the compressive side of the outer ring. The inner ring and outer ring shrink at roughly the same velocity for the armchair configuration. Thus the support from the inner tube to prevent the formation of ripples on the compressive side of the outer ring is weak. (V) If the diameter of the outermost wall of the multiwalled nanotube is the same as that of a single-walled nanotube, the formed multiwalled ring is more stable than the single-walled counterpart due to the support from the inner rings. For example, for an (8,8) single-walled nanotube without torsion, the critical diameter $D_C$ of the nanoring is approximately 20 nm. However, for a $(3,3)+(8,8)$ double-walled ring without torsion, the critical diameter $D_C$ is only 11.79 nm. This observation can be explained by the superlinear relation between the critical diameter of the ring and the tube diameter existing in single-walled rings shown in Fig. 1. This superlinear relation indicates that for the same ring diameter, the ring with the smaller tube diameter is more stable, thus the inner ring is able to provide support to the outer ring in a multiwalled nanotube.

Usually the wall-wall spacing in a multiwalled carbon nanotube is assumed to be the equilibrium value, that is, 0.34 nm.[24–28] In the present simulation, the effect of the wall-wall spacing on the stability of multiwalled rings was also investigated. It was found that the wall-wall distance also affects the stability of the double-walled nanorings, as indicated in Table I. For armchair configurations with diameters of 11.79 and 15.72 nm, the ring is stable only when the wall-wall distance is in the range of 0.20–0.34 nm, that is, equal to or slightly smaller than the equilibrium distance. When the wall-wall distance is outside this range, no stable rings were obtained in the present simulations. This observation applies to armchair rings both with and without torsion. For the zigzag nanorings with a ring diameter of 11.79 nm, the ring is stable when the wall-wall distance is in the range of 0.27–0.39 nm, that is, slightly lower or higher than the equilibrium distance. This result should be anticipated since multiwalled carbon nanotubes are most stable around their equilibrium wall-wall spacing.

The stability of triple-walled carbon nanorings was also examined in the present study and the comparison of single-, double-, and triple-walled rings was made. The following configurations were used: the (3,3), $(3,3)+(8,8)$, and $(3,3)+(8,8)+(13,13)$ rings with an armchair configuration and the (5,0), $(5,0)+(14,0)$, and $(5,0)+(14,0)+(23,0)$ rings with a zigzag configuration. It should be noted that the equilibrium wall-wall spacing was used. The effect of torsion was also considered in the present simulations. Figure 3 shows the relationship of the critical diameter $D_C$ of the nanorings versus the number of walls $N_w$. Generally, it can be seen that the critical diameter $D_C$ increases with an increase in the number of walls. This result can also be explained by the superlinear relationship between the ring diameter and the tube diameter in the single-walled cases, as shown in Fig.

TABLE I. The effect of the wall-wall spacing on the stability of double-walled rings.

| Type | Configuration | Diameter of nanorings (nm) | Wall-wall spacing (nm) | Stable |
|---|---|---|---|---|
| Armchair without torsion | (3,3)+(4,4) | $D$=11.79 | 0.067 | No |
| | (3,3)+(5,5) | | 0.136 | No |
| | (3,3)+(6,6) | | 0.203 | Yes |
| | (3,3)+(7,7) | | 0.271 | Yes |
| | (3,3)+(8,8) | | 0.339 | Yes |
| | (3,3)+(9,9) | | 0.407 | No |
| | (3,3)+(10,10) | | 0.475 | No |
| | (4,4)+(5,5) | $D$=15.72 | 0.067 | No |
| | (4,4)+(6,6) | | 0.136 | No |
| | (4,4)+(7,7) | | 0.203 | Yes |
| | (4,4)+(8,8) | | 0.271 | Yes |
| | (4,4)+(9,9) | | 0.339 | Yes |
| | (4,4)+(10,10) | | 0.407 | No |
| | (4,4)+(11,11) | | 0.475 | No |
| Armchair with torsion | (3,3)+(4,4) | $D$=15.72 | 0.067 | No |
| | (3,3)+(5,5) | | 0.136 | No |
| | (3,3)+(6,6) | | 0.203 | Yes |
| | (3,3)+(7,7) | | 0.271 | Yes |
| | (3,3)+(8,8) | | 0.339 | Yes |
| | (3,3)+(9,9) | | 0.407 | No |
| | (3,3)+(10,10) | | 0.475 | No |
| Zigzag without torsion | (5,0)+(7,0) | $D$=11.79 | 0.078 | No |
| | (5,0)+(8,0) | | 0.117 | No |
| | (5,0)+(10,0) | | 0.196 | No |
| | (5,0)+(12,0) | | 0.274 | Yes |
| | (5,0)+(14,0) | | 0.352 | Yes |
| | (5,0)+(15,0) | | 0.391 | Yes |
| | (5,0)+(16,0) | | 0.431 | No |
| | (5,0)+(17,0) | | 0.470 | No |

1. In addition, we found that for triple-walled rings, the zigzag configuration is more stable than its armchair counterpart, and the torsion has a destabilizing effect; these observations are consistent with those of (III) and (IV) for double-walled rings.

It was found that a series of events occurs during the relaxation of the multiwalled nanorings. The diameter of the nanoring shrinks gradually, accompanied by a change in the cross-sectional shape along the circumferential direction of the nanoring. The diameter and cross section will eventually be stabilized for a stable ring. Figures 4(a)–4(c) show the cross sections for the following three stable double-walled armchair rings without torsion: (4,4)+(9,9) with $D$ =15.72 nm, (5,5)+(10,10) with $D$=19.65 nm, and (6,6) +(11,11) with $D$=19.65 nm. It is seen that the flattened compressive and tensile parts of the inner tube walls are nearly parallel to each other while the cross section of the outer tube of the nanoring approaches an approximately elliptical shape. The flattened cross section is an effective structure to reduce the bending stiffness and stress, and hence the inner tube should be more flexible and less likely to suffer failure.

The present results show that if the nanoring is unstable, ripples first develop on the compressive side of the outermost tube, subsequently a small number of ripples develop into buckles, while a large number of the ripples disappear. This process is similar to the previous studies for single-walled nanorings.[10–14,29] Figure 5 shows a typical unstable deformation sequence during the energy relaxation of the double-walled armchair (5,5)+(10,10) nanoring with an initial diameter of $D$=11.79 nm without torsion. Figures 5(a)–5(c) show the deformation process of the inner tube while Figs. 5(d)–5(f) show the deformation process of the outer tube. One can see that, by comparing the initial configurations shown in Figs. 5(a) and 5(d) and the relaxed configurations shown in Figs. 5(b) and 5(e) the diameter of the nanoring shrinks markedly. Ripples develop on the compressive side

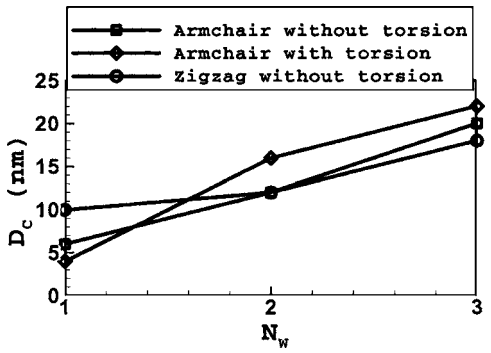


FIG. 3. The relationship of the critical diameter $D_C$ of the nanoring vs the number of walls $N_W$.

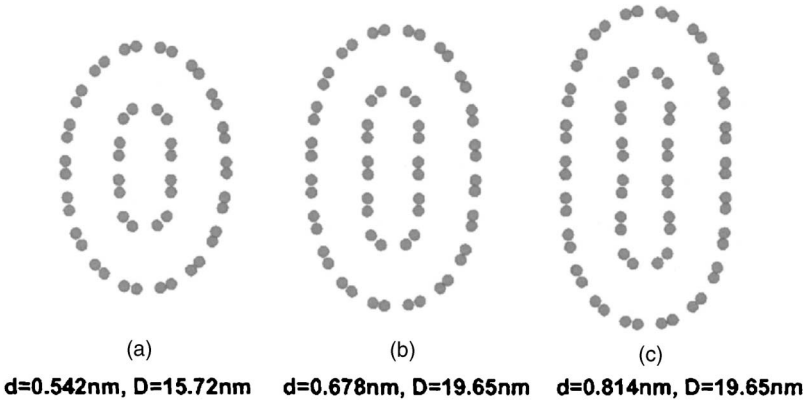


FIG. 4. The final stable cross sections for different nanotube configurations and nanoring diameters $D$ after relaxation. (a) $(4,4)+(9,9)$ with $D=15.72$ nm, (b) $(5,5)+(10,10)$ with $D=19.65$ nm, and (c) $(6,6)+(11,11)$ with $D=19.65$ nm.

of the outer tube, as shown in Fig. 5(e), the ripple formation was also observed in multiwalled nanotubes subjected to lateral bending.[25,28,30] Subsequently, buckles develop, as shown in Fig. 5(f), and finally cause failure in both inner and outer rings, as shown in Figs. 5(c) and 5(f). A similar unstable deformation sequence can also be found for both armchair and zigzag configurations, with and without torsion. However, it was found that the inclusion of torsion reduces the number of ripples at the compressive side of the outer ring. This can be clearly seen from Fig. 6 for the $(4,4)+(9,9)$ ring with an initial diameter of $D=11.79$ nm with torsion. For unstable nanorings with the same nanotube diameter, it was found that the number of ripples $N$ in the outermost tube increases approximately linearly with an increase in the diameter $D$ of the nanoring. This can be clearly seen from Fig. 7 (and its inset) for the $(5,5)+(10,10)$ configuration without torsion. Apparently the failure process during the formation of multiwalled rings is a complicated process deserving more future work.

Analytical solutions were obtained very recently for the critical buckling strain and wavelength of multiwalled carbon nanotubes under both axial compression and bending, based on a molecular mechanical model.[31] It will be interesting to compare the present results with the analytical ones. For the $(5m,5m)$ multiwalled nanotubes, where $m\in[1,M]$, the critical buckling strain under bending can be approximated as $0.111\ \text{nm}/(d_M+0.339\ \text{nm})$, where $d_M$ is the diameter of the outermost tube and $M$ is the total number of walls. For the $(5,5)+(10,10)$ double-walled nanotube, the analytical solution predicts that the buckling strain is 0.065. In the present calculation, the critical buckling strain is only 0.046. If the flattening of the cross-section a shape is ignored, the calculated critical buckling strain is roughly 0.062, which is close to the above analytical value. Thus the reason for this discrepancy is the flattening of the cross-sectional shape and possibly the nonlinear elastic deformation, since the nonlinearity and flattening of the cross section were not considered in the analytical solutions. In addition, the wavelength during buckling from the analytical solution is approximately equal to $\sqrt{0.385d_M}$ nm. For the $(5,5)+(10,10)$ double-walled nanotube, the analytical solution predicts that the critical wavelength is 1.02 nm. However, the critical wavelength in the present simulations depends on the initial ring diameter. For example, the critical wavelengths for diameters $D=7.86$ nm, $D=11.79$ nm, and $D=15.72$ nm are 0.77, 0.88, and 0.95 nm, respectively. Hence it appears that for an un-

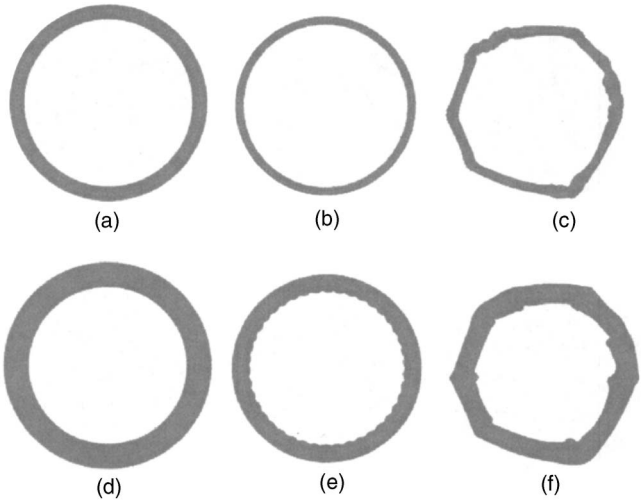


FIG. 5. The deformation sequence of a $(5,5)+(10,10)$ nanoring with an initial diameter of $D=11.79$ nm without torsion. During energy relaxation, the ring diameters shrink markedly. The ripples first develop on the compressive side of the outer wall, and subsequently buckle causing the failure of the ring.

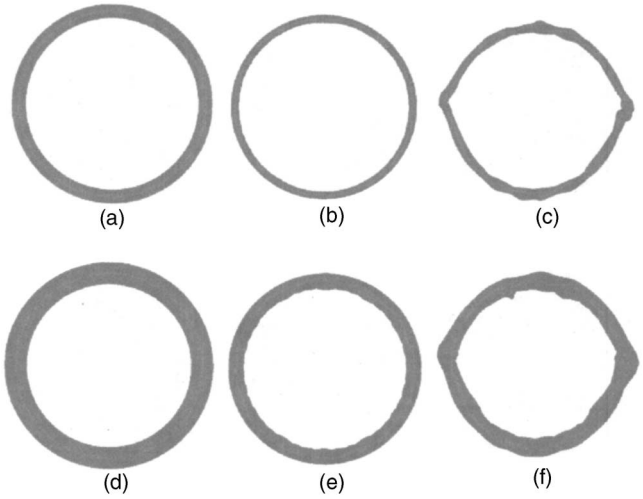


FIG. 6. The deformation sequence of a $(4,4)+(9,9)$ nanoring with an initial diameter of $D=11.79$ nm with torsion. The failure process is similar to the $(5,5)+(10,10)$ case. However, the ripple density along the circumferential direction is reduced with the inclusion of torsion.

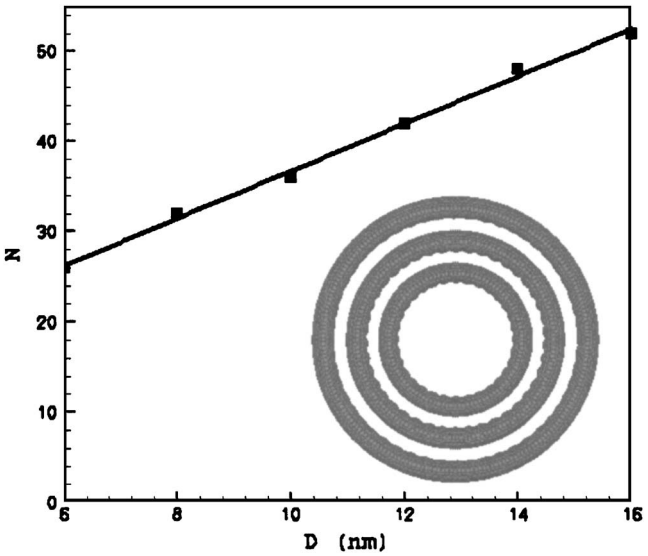


FIG. 7. The number of ripples $N$ of the outer tube vs the nanoring diameter $D$ of the $(5,5)+(10,10)$ type without torsion. The diameters of the nanorings in the inset are 7.86, 11.79, and 15.72 nm.

stable $(5,5)+(10,10)$ ring, the calculated critical wavelength gradually approaches the analytical value when the ring diameter increases.

## CONCLUSIONS

Atomistic simulations were performed to investigate the structure and stability of defect-free multiwalled carbon toroidal nanorings. It was found that the critical diameter for a stable nanoring depends on the system parameters, such as the number of walls, the wall-wall distance, the diameter, length, helicity, and torsion of the nanotubes. Several features concerning the stability of single-walled and multiwalled rings were compared. It was found that the instability of a multiwalled nanoring always starts with the formation of short-wavelength ripples on the compressive side of the outermost tube. Subsequently, some ripples will develop into buckles, resulting in buckling failures.

[1] R. H. Baughman, A. A. Zakhidov, and W. A. de Heer, Science **297**, 787 (2002).
[2] R. C. Haddon, Nature (London) **388**, 31 (1997).
[3] V. Meunier, P. Lambin, and A. A. Lucas, Phys. Rev. B **57**, 14886 (1998).
[4] J. Liu, H. J. Dai, J. H. Hafner, D. T. Colbert, R. E. Smalley, S. J. Tans, and C. Dekker, Nature (London) **385**, 780 (1997).
[5] R. Martel, H. R. Shea, and P. Avouris, Nature (London) **398**, 299 (1999).
[6] R. Martel, H. R. Shea, and P. Avouris, J. Phys. Chem. B **103**, 7551 (1999).
[7] M. Ahlskog, E. Seynaeve, R. J. M. Vullers, C. Van Haesendonck, A. Fonseca, K. Hernadi, and J. B. Nagy, Chem. Phys. Lett. **300**, 202 (1999).
[8] M. Sano, A. Karnino, J. Okamura, and S. Shinkai, Science **293**, 1299 (2001).
[9] J. F. Colomer, E. Henrard, E. Flahaut, G. Van Tendeloo, A. A. Lucas, and Ph. Lambin, Nano Lett. **3**, 685 (2003).
[10] L. Liu, C. S. Jayanthi, and S. Y. Wu, Phys. Rev. B **64**, 033412 (2001).
[11] J. Han, Chem. Phys. Lett. **282**, 187 (1998).
[12] M. Huhtala, A. Kuronen, and K. Kaski, Comput. Phys. Commun. **146**, 30 (2002).
[13] M. Huhtala, A. Kuronen, and K. Kaski, Comput. Phys. Commun. **147**, 91 (2002).
[14] O. Hod, E. Rabani, and R. Baer, Phys. Rev. B **67**, 195408 (2003).
[15] D. H. Oh, J. M. Park, and K. S. Kim, Phys. Rev. B **62**, 1600 (2000).
[16] V. Meunier, P. Lambin, and A. A. Lucas, Phys. Rev. B **57**, 14886 (1998).
[17] S. L. Zhang, S. M. Zhao, M. G. Xia, E. H. Zhang, and T. Xu, Phys. Rev. B **68**, 245419 (2003).
[18] S. M. Zhao, S. L. Zhang, M. G. Xia, E. H. Zhang, and X. J. Zuo, Phys. Lett. A **331**, 238 (2004).
[19] L. F. Yang, J. Jiang, and J. M. Dong, Phys. Status Solidi B **238**, 115 (2003).
[20] L. F. Yang, J. W. Chen, and J. M. Dong, Phys. Status Solidi B **241**, 1269 (2004).
[21] D. W. Brenner, O. A. Shenderova, J. A. Harrison, S. J. Stuart, B. Ni, and S. B. Sinnott, J. Phys.: Condens. Matter **14**, 783 (2002).
[22] Y. Wang, D. Tomanek, and G. F. Bertsch, Phys. Rev. B **44**, 6562 (1991).
[23] O. A. Shenderova, D. W. Brenner, A. Omeltchenko, X. Su, and L. H. Yang, Phys. Rev. B **61**, 3877 (2000).
[24] P. Liu, Y. W. Zhang, and C. Lu, Appl. Phys. Lett. **85**, 1778 (2004).
[25] O. Lourie, D. M. Cox, and H. D. Wagner, Phys. Rev. Lett. **81**, 1638 (1998).
[26] P. Poncharal, Z. L. Wang, D. Ugarte, and W. A. de Heer, Science **283**, 1513 (1999).
[27] S. Iijima, C. Brabec, A. Maiti, and J. Bernholc, J. Chem. Phys. **104**, 2089 (1996).
[28] A. Pantano, M. C. Boyce, and D. M. Parks, Phys. Rev. Lett. **91**, 145504 (2003).
[29] C. Li and W. L. Guo, Int. J. Nonlinear Sci. Numer. Simul. **4**, 387 (2003).
[30] J. Z. Liu, Q. S. Zheng, and Q. Jiang, Phys. Rev. B **67**, 075414 (2003).
[31] T. C. Chang, W. L. Guo, and X. M. Guo, Phys. Rev. B **72**, 064101 (2005).